Fluid Mechanics
2020; 6(2): 51-61
http://www.sciencepublishinggroup.com/j/fm
doi: 10.11648/j.fm.20200602.12
ISSN: 2575-1808 (Print); ISSN: 2575-1816 (Online)

Analysing the Effects of Non-newtonian Viscoelastic Fluid Flows on Stretching Surfaces with Suction

Golbert Aloliga[1, *], Isaac Azuure[2]

[1]Department of Mathematics, St Vincent College of Education, Tamale, Ghana

[2]Department of Computer Science, Regentropfen College of Applied Sciences, Bolga, Ghana

Email address:

aloligagolbert@gmail.com (G. Aloliga), azureike@yahoo.com (I. Azuure)

[*]Corresponding author

To cite this article:

Golbert Aloliga, Isaac Azuure. Analysing the Effects of Non-newtonian Viscoelastic Fluid Flows on Stretching Surfaces with Suction. *Fluid Mechanics*. Vol. 6, No. 2, 2020, pp. 51-61. doi: 10.11648/j.fm.20200602.12

Received: December 14, 2019; **Accepted**: December 30, 2019; **Published**: August 27, 2020

Abstract: The fourth order Runge-Kutta integration scheme coupled with numerical shooting algorithm is employed to examine heat and mass transfer in a steady two-dimensional Magnetohydrodynamic non-Newtonian fluid flow over a stretching vertical surface with suction by considering radiation, viscous dissipation, Soret and Dufour effects. A steady two-dimensional magneto hydrodynamic non-Newtonian fluid flow over a flat surface with suction has been studied. The boundary layer governing partial differential equations are derived by considering the Bossiness approximations. These equations are transformed to nonlinear ordinary differential equations by the techniques of similarity variables and are solved analytically in the presence of buoyancy forces. The effects of different parameters such as magnetic field parameter, Prandtl number, buoyancy parameter, Soret number, Dufour number, radiation parameter, Brinkmann number, suction parameter and Lewis number on velocity, temperature, and concentration profiles are presented graphically and in tables and discussed quantitatively. Results show that the effect of increasing Soret number or decreasing Dufour number tends to decrease the velocity and temperature profiles (increase in Soret cools the fluid and reduces the temperature) while enhancing the concentration. Among the many importance of the fluid in chemical engineering, metallurgy, polymer extrusion process will definitely require cooling the molten liquid to further cool the system, for the production of paper and glass. In this process, the rate of cooling and shrinking influences very much on the final quality of the product.

Keywords: Viscoelastic Fluids, Mass Transfer, Non-newtonian Fluid, Stretching Surfaces, Suction

1. Introduction

The research seeks to investigate the dynamics of hydromagnetic boundary layer flow of non-Newtonian fluids which has attracted much attention in industrial applications. The intension is to control the flow kinematics of fluid with the application of magnetic fields a process called magneto hydrodynamics (MHD).

In MHD flow, the magnetic field is used to change the velocity and pressure characteristics of the flow and can also significantly delay the onset of turbulent fluctuations. These effects together or individually can dramatically alter the heat and mass transfer characteristics and hence the fluid drags on the surface. Fluids having better electromagnetic properties are normally used in cooling liquid, since imposing a magnetic field on it can control its velocity to improve quality product examined by [1].

Applications of such phenomena include cooling systems for magnetic fusion reactors and reduced-drag ship hulls and airplane fuselages. The MHD force can be applied in such a way that useful work can be done. The obstacle to a workable theory of fluid mechanics is the action of viscosity, which can be neglected only in certain idealized flows.

Viscosity is a measure of a fluid's resistance to flow. Viscous materials are thick or sticky and can act as adhesive. Fluid with large viscosity resists motion but fluid with low viscosity flows easily. For instance, water has low viscosity so it flows easier than honey which relatively, has a high viscosity. Some highly viscous materials include honey, syrups, tooth paste and gels. A fluid in which the viscous stresses arising from its flow at every point are

linearly proportional to the rate of change in its deformation over time is called Newtonian fluid. On the other hand, a fluid whose flow properties differ in any way from those of the Newtonian fluid is called a non-Newtonian fluid. Most commonly, the viscosity of Newtonian fluids is dependent on shearrate or shear rate history. In a Newtonian fluid, the relation between the shear stress and the shear rate is linear with the constant of proportionality being the coefficient of Viscosity is observed to have some bearings on the fluid flow kinematics. In reality, some fluids have complex viscosities than others. Fluids whose shear stresses are linearly proportional to the velocity gradient are called Newtonian fluids, otherwise they are non-Newtonian. A special type is the viscoelastic fluid which exhibits both viscous and elastic behavior when deformed. The purpose of the study of this special fluid cannot be overlooked due to its increasing importance in industries. Many vigorous studies have been done on viscoelastic fluid flow over stretching boundary.

Similarly, first to investigate MHD flows problem of electrically conducting viscoelastic fluid past a flat and impermeable elastic sheet has been explained in [2]. He further examined the influence of uniform magnetic field on the motion of an electrically conducting fluid past a flat and impermeable elastic sheet and obtained closed form solutions of the momentum boundary layer equation. His work was extended by many authors, such as [3, 4] who included other thermo-physical parameters. They all realized that the viscoelasticity of the fluid had a strong influence on the flow velocity. Similarly,[5] investigated similarity solutions for hydromagnetic simultaneous heat and mass transfer by natural convection from an inclined plate with internal heat generation or absorption. The unsteady MHD convective heat transfer past a semi-infinite vertical porous moving plate with variable suction has been reported by [6].

MHD visco-elastic fluid flow over a continuously moving vertical surface with chemical reaction was examined by [7]. The present visco-elastic fluid model works to suggest rheological liquids encountered in biotechnology (medical creams) and chemical engineering. [8] then analyzed the thermal radiation and buoyancy effects on MHD free convective heat generation flow over an accelerating permeable surface with temperature dependent viscosity. In all these works, it was observed that the heat transfer on hydromagnetic flow depended on the thickness (viscosity) of the fluid under consideration.

Dufour and Soret effects have been known to many researchers over time. When heat and mass transfer occur in a moving fluid, the energy flux can be generated by a composition gradient, namely, the Dufour or diffusion-thermo effects, and the mass fluxes developed by the temperature gradients called the Soret or thermal-diffusion effects [9]. Meanwhile, some researchers have neglected the Dufour and Soret effects on heat and mass transfer according to Fourier's and Fick's laws. When density differences exist in the flow regime, these effects are important and should not be neglected. Again [10] studied the influence of transverse magnetic field on the flow and heat transfer in an electrically conducting second grade fluid over a stretching sheet subject to suction. whilst [11] investigated the viscoelastic MHD flow and heat transfer over a stretching sheet with viscous and ohmic dissipation and [12] investigated the effects of joule heating and viscous dissipation of mixed convection MHD flow in vertical channels whilst [13] theoretically investigated the steady MHD free convection and mass transfer of an electrically conducting fluid through a porous medium. It was realized that varying conditions of the surface of flow-like stretching as encountered in polymer extrusion or porosity as in manufacturing of textiles affect the rate at which heat and mass are transferred. Some researchers have been led by this to include various physical aspects of the problem of combined heat and mass transfer examined by [14] while [15] considered the thermal radiation and an exponentially-stretching surface for the boundary layer. The boundary layer flow due to a shrinking sheet is emerged as an interesting problem in fluid dynamics. (MHD) boundary layer flow and combined heat and mass transfer of a non-Newtonian fluid over an inclined stretching sheet was investigated by [16] while [17] discussed the analysis of thermal boundary layer in the flow of Casson fluid over a permeable shrinking sheet with variable wall temperature and thermal radiation. The boundary layer flow of Casson fluid over a permeable stretching/shrinking sheet with magnetic field effect was recently investigated by [18].

Soon after his investigation, [19] critically examined MHD boundary layer flow of casson fluid over a Stretching/shrinking sheet through porous medium. He observed that velocity of the fluid will increase, when the magnetic parameter, the casson parameter on the shrinking sheet decreases and increasing the velocity of the fluid, will have to decrease the magnetic parameter and the casson parameter on the stretching sheet.

Grease as an important lubricant in modern tribological systems was stuied by [20]. Yet modelling these fluids in thin lubricating films is hard due to the discontinuities in the rheological properties caused by the yield stress. A good method to model this behavior was especially relevant in the design of bearings using Magneto- or Electrorheological fluids according to [21].

A workable improved particle shifting technique for incompressible smoothed particle hydrodynamics method was investigated by [22]. The particle shifting technique (PST) based on Fick's law was an efficient one. The method was validated by modeling different cases including dam break flow, paddle movement and elliptical water drop. The method furthermore starts with an assumed surface stress value, which is iteratively modified to match the given surface velocity. The impacts of entropy generation and Hall current on MHD Casson, a non-Newtonian fluid over a stretching Surface with velocity slip factor have been numerically analyzed [23].

The last three decades have seen an increase in the interest of MHD free or mixed convection from a plate embedded in porous media. This is largely due to its application in

industry involving heat exchanger design, petroleum production, filtration, chemical catalytic reactors, and MHD generators. Other applications of free convection in engineering include heat rejection into the environment such as in water bodies like lakes, rivers and the sea. Thermal energy storage systems such as solar ponds and condenser of power plants are common examples.

In this study, the combined effect of Radiation and viscous dissipation in a hydromagnetic fluid flow with convective boundary conditions considering the effects of Dufour and Soret are investigated.

2. Mathematical Model

Consider a steady two-dimensional heat and mass transfer flow of an incompressible electrically conducting viscoelastic fluid with k_0 as the viscoelasticity parameter, over a stretching vertical surface with a variable magnetic field $B(x) = B_0 x^{(n-1)/2}$ normally applied to the surface (Figure 1). With fixed origin, two equal and opposite forces are applied along the x-axis. It is assumed that the stretching velocity is $u_w(x) = ax^n$, where a and n are constants. The induced magnetic field is neglected in comparison to the applied magnetic field and the viscous dissipation is small. The governing equations subject to Boussinesq approximation, the boundary-layer assumptions, and the above assumptions will be considered to formulate the problem.

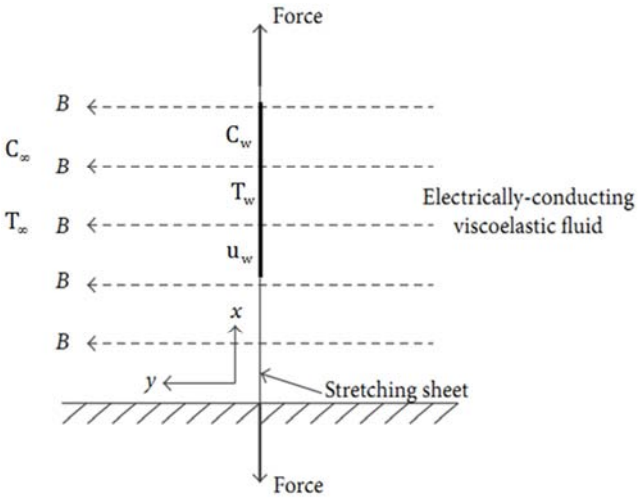

Figure 1. *A pictorial display of the study problem.*

Let the *x*-axis be taken along the direction of the plate and *x*-axis normal to it. If *u*, *v*, *T*and *C* are the fluid *x*-component of velocity, *y*-component of velocity, temperature and concentration respectively. With these assumptions, the governing equations for the problem can be modeled as:

$$\frac{\partial u}{\partial x}+\frac{\partial v}{\partial y}=0 \tag{1}$$

$$\left(u\frac{\partial u}{\partial x}+v\frac{\partial u}{\partial y}\right)=-\frac{1}{\rho}\frac{\partial p}{\partial x}+\frac{\mu}{\rho}\frac{\partial^2 u}{\partial y^2}+\rho g \tag{2}$$

$$u\frac{\partial u}{\partial x}+v\frac{\partial u}{\partial y}=\upsilon\frac{\partial^2 u}{\partial y}+k_0\left\{u\frac{\partial^3 u}{\partial x\partial y^2}+v\frac{\partial^3 u}{\partial y^3}+\frac{\partial u}{\partial x}\frac{\partial^2 u}{\partial y^2}+\frac{\partial u}{\partial y}\frac{\partial^2 u}{\partial x\partial y}\right\}+g\beta_t(T-T_\infty)+g\beta_c(C-C_\infty)-\frac{\sigma B^2(x)}{\rho}u, \tag{3}$$

$$u\frac{\partial T}{\partial x}+v\frac{\partial T}{\partial y}=\alpha\frac{\partial^2 T}{\partial y^2}+\frac{\upsilon}{c_p}\left(\frac{\partial u}{\partial y}\right)^2+\frac{D_m\kappa_T}{c_s c_p}\frac{\partial^2 C}{\partial y^2}-\frac{\alpha}{\kappa}\frac{\partial q_r}{\partial y} \tag{4}$$

subject to the following boundary conditions:

$$\begin{aligned} &y=0: u=u_w(x),\ v=v_w,\ T=T_w(x),\ C=C_w(x),\\ &y\to\infty: u\to 0,\ \frac{\partial u}{\partial y}\to 0,\ T\to T_\infty,\ C=C_\infty. \end{aligned} \tag{5}$$

Where *u*, *v*, *T*and *C* are the fluid *x*-component of velocity, *y*-component of velocity, temperature and concentration respectively where ρ is the density of the fluid, g is the acceleration due to gravity, p is the external pressure and μ is the dynamic viscosity of the fluid, q_r is the radiative heat flux, D is the mass diffusivity and $\dot{r}$ is the rate of species generation or destruction, υ is the kinematic viscosity and *t*is time, $\delta_m \approx 2\sqrt{\upsilon t}$ is the momentum boundary layer thickness, $u_w(x) = ax^n$, is the stretching velocity where a and n are constants, $\eta = y\sqrt{\frac{ax^{n-1}}{v}}$is the similarity parameter, $\psi = \sqrt{av x^{n+1}} f(\eta)$ is the steam function, $f' = \frac{u}{u_w}$, $\theta = \frac{T-T_\infty}{T_s-T_\infty}$, $\varphi = \frac{C-C_\infty}{C_s-C_\infty}$ is the dimensionless velocity, temperature and concentration respectively, $Q = W\psi$, is the volumetric flow. The following dimensionless quantities are introduced:

$$u=\frac{\partial\psi}{\partial y}=\sqrt{a\upsilon x^{n+1}}\cdot\sqrt{\frac{ax^{n-1}}{\upsilon}}f'=ax^n f'$$

$$v=-\left\{\frac{n+1}{2}\sqrt{a\upsilon x^{n-1}}f+\frac{a(n+1)}{2}yx^{n-1}f'\right\}$$

$$f'=\frac{u}{u_w},\ \theta=\frac{T-T_\infty}{T_s-T_\infty},\ \varphi=\frac{C-C_\infty}{C_s-C_\infty} \tag{6}$$

Substituting equation (6) in (1) – (5) gives:

$$nf'^2 - \frac{(n-1)}{2} ff'' = f''' + k_1 \left\{ (3n-1) f f''' - \frac{3n-1}{2} f''^2 - \frac{n-1}{2} f f'''' \right\} - Mf' + \lambda(\theta + \mathrm{N}\varphi) \quad (7)$$

$$\left(1 + \frac{4}{3} Ra\right)\theta'' + \Pr\left(\frac{n+1}{2} f\theta' - f'\theta + Du\varphi''\right) = 0. \quad (8)$$

$$\varphi'' + Le\left\{\Pr\left(\frac{n+1}{2} f\varphi' - f'\varphi\right) + Sr\theta''\right\} = 0. \quad (9)$$

The transformed boundary conditions are

$$f(0) = fw, f'(0) = 1, \theta(0) = 1, \phi(0) = 1, f'^{(\infty)} = 0, f''(\infty) = 0, \theta(\infty) = 0, \phi(\infty) = 0 \quad (10)$$

3. Numerical Procedure

This method explores various findings obtained through the mathematical analysis of the dimensionless coupled governing equations in (7-9) and the associated boundary conditions (10). An efficient and robust numerical method based on the shooting technique along with the fourth-order Runge-Kutta integration algorithm is employed for the solution of the ode resulting from model transformation. Before applying the numerical methods, the model is first reduced partial differential equations to a coupled first order system of ordinary differential equation

To select a representative value for the infinity the similarity value can assume (η_∞,), we begin with some initial guess value and solve the problem with some particular set of parameters to obtain f "(0), θ'(0) and $\phi'(0)$. The solution process is repeated with another larger value of η_∞ until two successive values of f"(0), θ'(0) and $\phi'(0)$ differ only after desired digit signifying the limit of the boundary along η. The last value of η_∞ is chosen as appropriate value for that particular simultaneous equation of first order for seven unknowns following the method of superposition. To solve this system we require seven initial conditions whilst we have only two initial conditions $f'(0)$ and $f(0)$ on f; and one initial condition each on θ and ϕ. This means that there are three initial conditions, f"(0), θ'(0) and $\phi'(0)$ which are not prescribed. Now, we employ numerical shooting technique where these two ending boundary conditions are utilized to produce two unknown initial conditions at η=0. In this calculation, the step size $\Delta\eta$=0.001 was used while obtaining the numerical solution with $\eta_{\max}$=10 and six-decimal (10^{-6}) accuracy as the criterion for convergence. The numerical procedure was carried out using a Maple 16 software package. A representative set of numerical results are displayed graphically and discussed quantitatively to show some interesting aspects of some pertinent controlling parameters of the flow on the dimensionless axial velocity profiles, temperature profiles, concentration profiles, local skin friction coefficient, rate of heat transfer and the rate of mass transfer. The discussions of the results are also presented.

4. Results and Discussing

To ensure the accuracy of the applied numerical scheme, we compare our derived results corresponding to the skin-friction coefficient ($f''(0)$) and the local Nusselt number ($-\theta'(0)$) for steady viscoelastic fluid flow without any thermal radiation effect with the results in Table 1. The presentation indicates a perfect agreement to six decimal places.

Table 1. *Comparison of values of f"(0) and –θ'(0) for different values of Pr with M=0.1, Le=1, λ=0.6, k_1=1, Sr=0.25, Du=0.2, fw=0.1, N=-0.5.*

Pr	[24]		Present Study	
	$f''(0)$	$-\theta'(0)$	$f''(0)$	$-\theta'(0)$
0.72	0.6238107	0.8077915	0.623810688	0.807791568
1.00	0.6554146	0.9547582	0.655414606	0.954758266
4.00	0.7448565	1.3464869	0.744856500	1.346486897
7.20	0.7610054	0.3315818	0.761005380	0.331581797
10.00	0.7646628	1.9714629	0.764662786	1.971462891

Effects of Parameters on Skin Friction and the Rate of Heat and Mass Transfer

Table 2. *Results of skin friction coefficient, Nusselt and Sherwood numbers for various values of controlling parameters.*

Pr	M	Le	λ	k_1	fw	Ra	Sr	Du	$f''(0)$	$-\theta'(0)$	$-\varphi'(0)$
0.72	0.5	1.0	0.6	1.0	0.1	0.1	0.25	0.2	0.578885	0.765660	0.779424
4.00									0.629798	1.300796	2.269188
7.10									0.630828	0.503268	3.416976

Pr	M	Le	λ	k_1	fw	Ra	Sr	Du	$f'(0)$	$-\theta'(0)$	$-\varphi'(0)$
	1.0								0.917888	0.692956	0.706529
	1.5								1.066446	0.662270	0.675693
		2.0							0.712387	0.698958	1.148993
		3.0							0.698136	0.666500	1.473655
			1.0						0.668377	0.746080	0.759811
			1.5						0.579928	0.762905	0.776689
				1.5					0.656353	0.752241	0.765951
				2.0					0.630828	0.503268	3.416976
					1.0				0.834552	0.970292	0.992196
					1.5				0.867677	1.125651	1.152787
						1.0			0.665802	0.485012	0.823452
						1.5			0.641150	0.422576	0.844215
							0.05	1.00	0.679120	0.465240	0.866557
							0.10	0.50	0.715211	0.632820	0.829525

The results of varying parameter values on the local skin friction coefficient, the local Nusselt number and the local Sherwood number, are shown in Table 2. It is observed that the skin friction increases with increasing values of Pr, M, and *fw*; and decreases with increasing values of Le, λ, Ra and k_1. This means that the combined effect of high viscosity over thermal diffusion, the induced Lorenz force, and suction at the surface of the sheet is to increase the local skin friction; and the combined effect of high thermal diffusion over mass diffusion, buoyancy forces, radiation and viscoelasticity of the fluid is to decrease the local skin friction at the surface of the plate. It is also observed that the effect of Soret (Sr) and Dufour (Du) numbers tends to increase the skin friction due to high temperature gradient.

Similarly, the rate of heat transfer at the plate surface increases with increase in parameter values of λ, *fw*and the effect of Sr and Du; and reduces with increasing values of Pr, *M, Le, k_1,* and *Ra*.

Moreover, it is observed that the rate of mass transfer increases with increasing values of Pr, Le, λ, k_1, *fw* and Ra; and decreases with increasing values of Mand the effect of Sr and Du.

5. Graphical Results

5.1. Effects of Parameter Variation on the Velocity Profiles

The effects of parameter variation on the velocity boundary layer are shown in Figures 2-9. The effect of magnetic parameter on the velocity is plotted in Figure 2. It is observed that the velocity decreases with increasing magnetic field intensity. This is due to the fact that the applied magnetic field normal to the flow induces a drag in terms of a Lorentz force which provides resistance to flow. Increase in Pr leads to increase in kinematic viscosity and velocity decreases. It is clearly shown that with the increase in Pr the velocity profiles reduce (Figure 3).

The governing equations are coupled together only with the buoyancy parameter (λ). When λ increases, the Grashof number accelerates the fluid so the velocity and the boundary-layer thickness increase, as shown in Figure 4. Increase in buoyancy enhances convection and leads to enhancement in velocity. This fact is also adequate to explain the observed increase in the velocity profile as a result of increasing the radiation parameter (*Ra*) as in Figure 9. We can note here that, increasing buoyancy forces will lead to a better flow kinematics.

The effect of varying values of the viscoelasticity parameter (k_1) on the velocity profile is shown in Figure 5. It is observed that increasing values of the k_1 lead to an infinitesimal increase at the velocity boundary layer thickness and hence slowing the flow velocity due to viscous and elastic effects.

The Soret effect (Sr) is a mass flux due to a temperature gradient and the Dufour effect (Du) is enthalpy flux due to a concentration gradient and appears in the energy equation. The effects of Sr and Du on velocity are shown in Figure 6. We considered the effects of Du and Sr so that their product remains constant at 0.05. As one can see the increase in the value of Sr or decrease in Du reduces the velocity.

Lewis number (Le) is the ratio of thermal diffusivity to mass diffusivity. Le can also be expressed as the ratio of the Schmidt number to the Prandtl number (Le=Sc/Pr). Figure 2 displays the effect of Le on the velocity profile. The effect of increasing the value of Le on the velocity is as the same as the effect of decreasing the value of Pr and it can be easily understood that with the enhancement of Le the velocity distribution increases.

For various values of suction parameter (*fw*), the profiles of the velocity across the boundary layer are shown in Figure 8. The velocity decreases for increasing values of *fw.* This can be attributed to the fact that suction is an agent which causes resistance to the fluid flow hence retarding the fluid velocity.

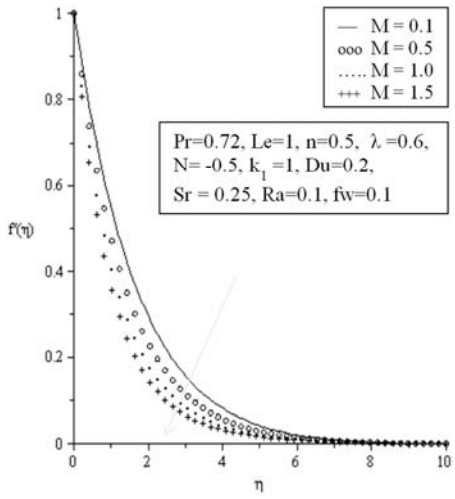

Figure 2. *Velocity profiles for varying values of magnetic field parameter (M).*

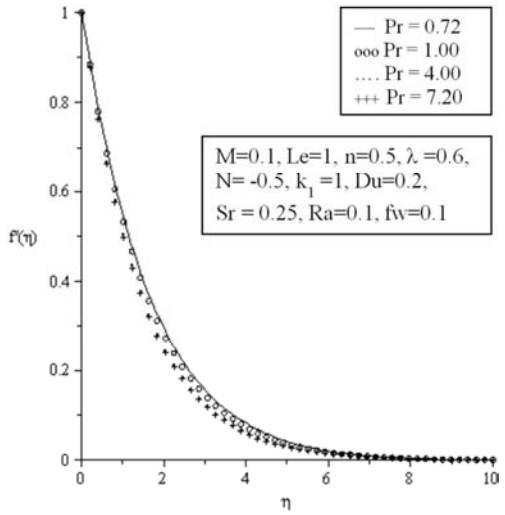

Figure 3. *Velocity profiles for varying values of Prandtl number (Pr).*

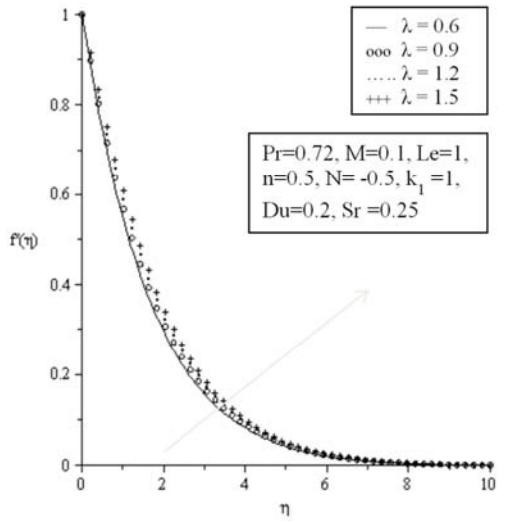

Figure 4. *Velocity profiles for varying values of buoyancy parameter (λ).*

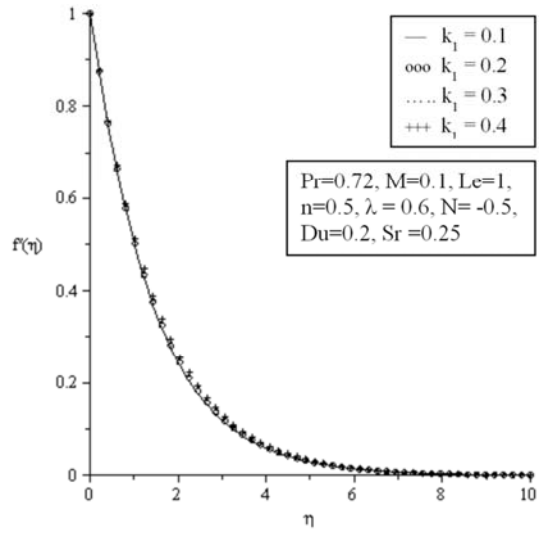

Figure 5. *Velocity profiles for varying values of viscoelasticity parameter (k_1).*

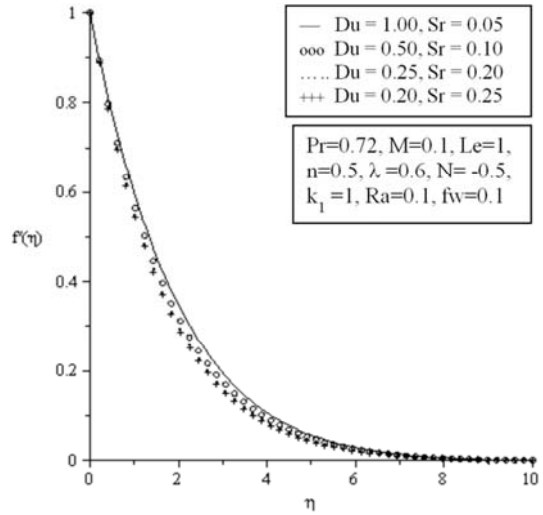

Figure 6. *Velocity profiles for varying values of Dufour (Du) and Soret (Sr) numbers.*

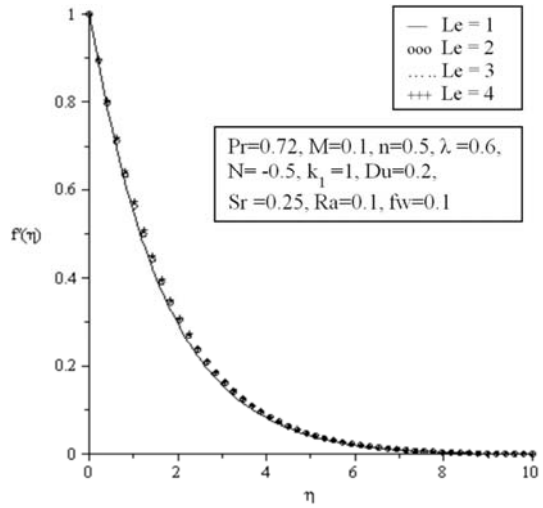

Figure 7. *Velocity profiles for varying values of Lewis number (Le).*

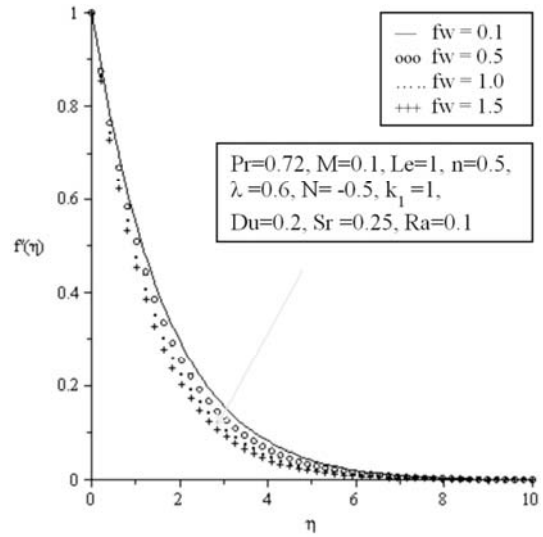

Figure 8. *Velocity profiles for varying values of suction parameter (fw).*

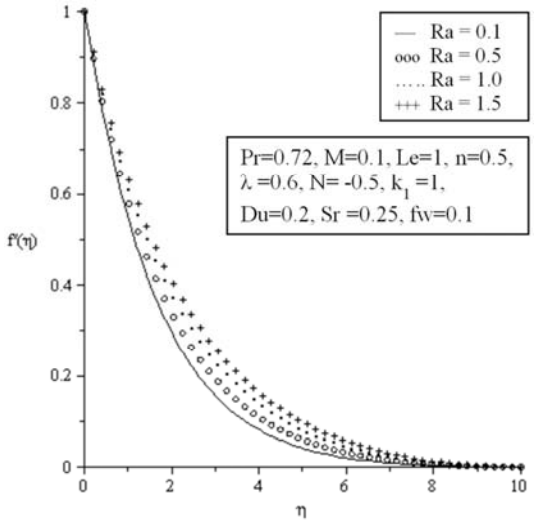

Figure 9. *Velocity profiles for varying values of radiation parameter (Ra).*

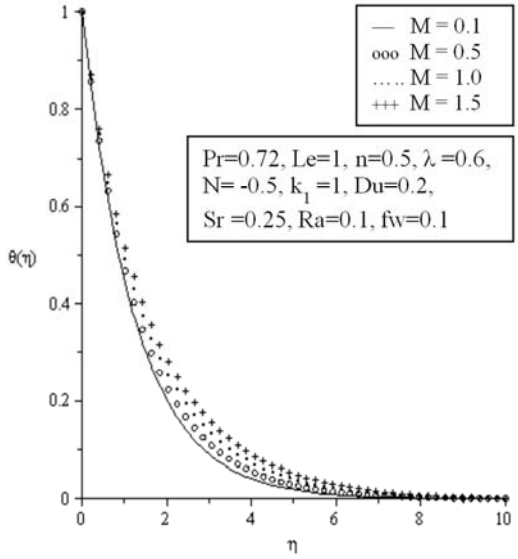

Figure 10. *Temperature profiles for varying values of magnetic parameter (M).*

5.2. Effects of Parameter Variation of Temperature Profiles

The effects of parameter variation on temperature profiles are shown in Figures 10 - 17. Figure 13 displays the variation of Prandtl number (Pr) on the temperature. In Figure 10 the effect of magnetic field parameter (M) on temperature profiles is illustrated. The magnetic effect causes skin-frictional heating and so the wall temperature increases and the thickness of thermal boundary-layer increases.

The effects of Prandtl number (Pr) on temperature distributions are illustrated in Figure 11. With the increase in Pr the thermal diffusion decreases, so the thermal boundary-layer becomes thinner and temperature decreases. A fluid with larger Pr and higher heat capacity increases the heat transfer. Again, this temperature decrease is reasonable in the sense that larger Prandtl number corresponds to the weaker thermal diffusivity and thinner boundary layer.

The effect of buoyancy parameter (λ) on temperature profile is shown in Figure 12. The thermal and concentration boundary-layer thicknesses decrease with the increase in the value of buoyancy parameter. It is observed in Figure 13 that increasing values of the viscoelasticity parameter tend to shrink the thermal boundary layer.

The effect of Soret (Sr) and Dufour (Du) numbers on temperature profile is shown in Figure 14. The increase in the value of Sr or decrease in Du causes the temperature profile to decline. Increase in Soret number cools the fluid and reduces the temperature. The effect of Lewis number (Le) on temperature profile is presented in Figure 15. The temperature decreases with the increase in Le similar to the results presented.

It is observed in Figure 16 that, increasing *fw* also reduces the temperature profile for obvious reasons. It is observed in Figure 17 that thermal radiation (Ra) increased the temperature profiles. This is due to the fact that as more heat is generated within the fluid, the fluid temperature increases leading to a sharp inclination of the temperature gradient between the plate surface and the fluid.

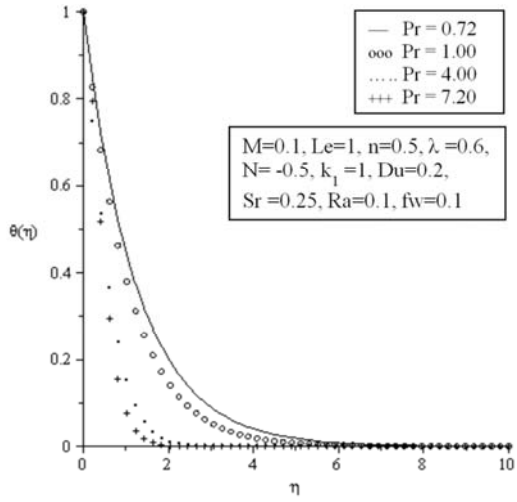

Figure 11. *Temperature profiles for varying values of Prandtl number (Pr).*

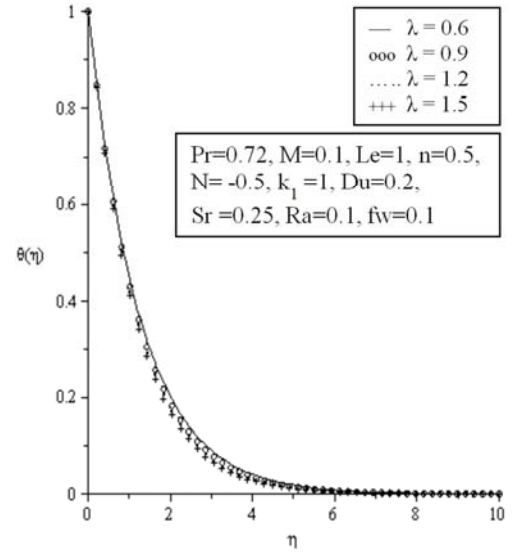

Figure 12. *Temperature profiles for varying values of buoyancy parameter (λ).*

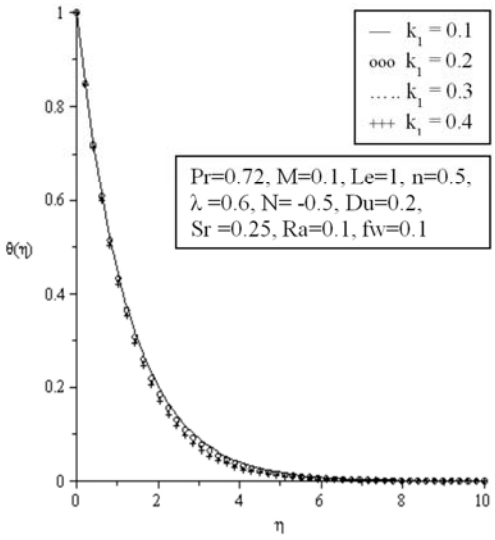

Figure 13. *Temperature profiles for varying values of viscoelasticity parameter (k_1).*

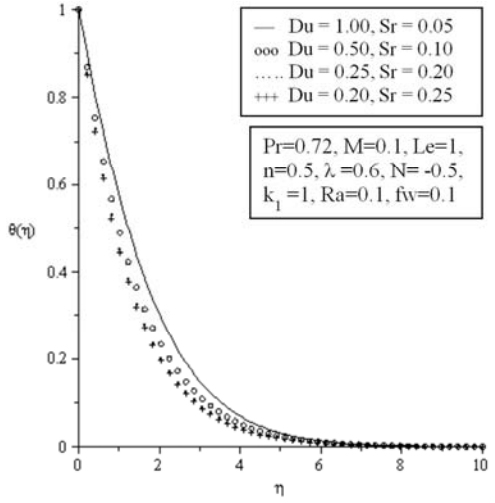

Figure 14. *Temperature profiles for varying Dufour (Du) and Soret (Sr) numbers.*

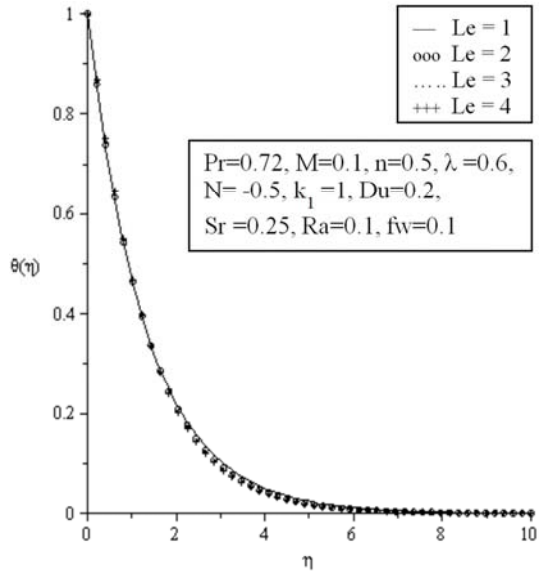

Figure 15. *Temperature profiles for varying values of Lewis number (Le).*

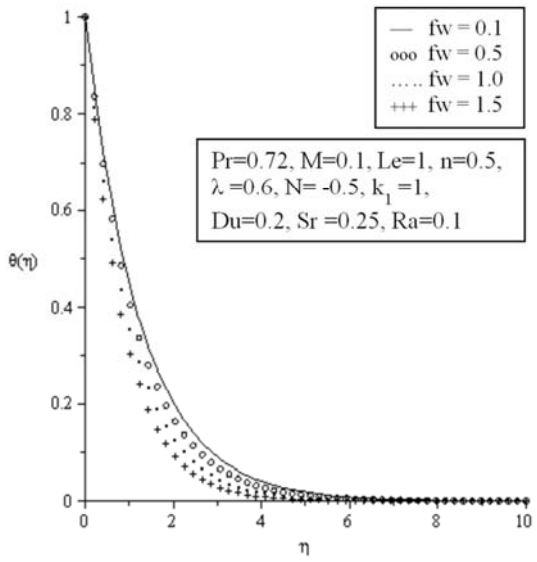

Figure 16. *Temperature profiles for varying values of suction parameter (fw).*

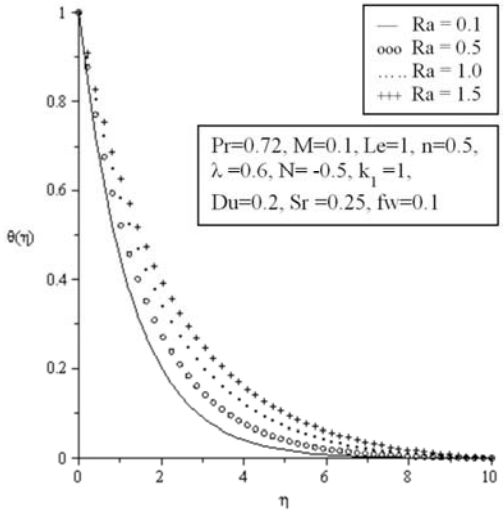

Figure 17. *Temperature profiles for varying values of radiation parameter (Ra).*

5.3. Effects of Parameter Variation on the Concentration Profiles

Figures 18-25 depict the effects of varying parameters on the concentration boundary layer thickness. The effect of magnetic field parameter (M) on concentration profile is shown in Figure 18. It can be seen that increase values of M is to increase the concentration profile.

The effects of Prandtl number (Pr) on concentration distribution is illustrated in Figure 19. The Pr reduces the concentration distribution just the same as its effect on temperature profile (Figure 11). The effect of Lewis number on concentration profile is presented in Figure 20. With the increase in Le the mass diffusivity decreases and the concentration descends. The effect of buoyancy parameter (λ) on concentration profile is shown in Figures 21. The thermal and concentration boundary-layer thicknesses decrease with the increase in the value of buoyancy parameter.

It is observed in Figure 22 that increasing values of the

viscoelasticity parameter tend to shrink the thermal boundary layer just the same as its effect on temperature profile (Figure 13). The effect of Soret (Sr) and Dufour (Du) numbers on concentration profile is shown in Figure 23. The increase in the value of Sr or decrease in Du causes concentration boundary layer to grow thick and enhances the concentration distribution.

Figure 24 illustrates the effect of suction parameter (*fw*) on the concentration profile. It is observed that the concentration boundary layer thickness reduces with increasing values *fw*. This is similar to what happens to the concentration boundary layer upon increasing the radiation parameter (Figure 25). This decrease in the concentration distribution can be concentration distribution is dispersed away largely due to increased temperature gradient.

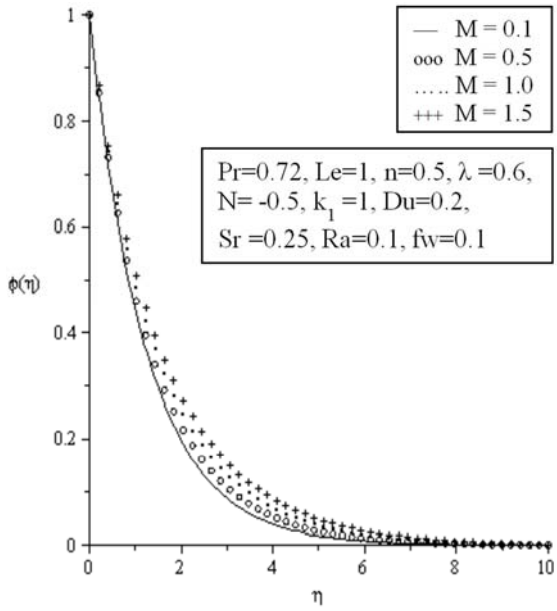

Figure 18. *Concentration profiles for varying values of magnetic parameter (M).*

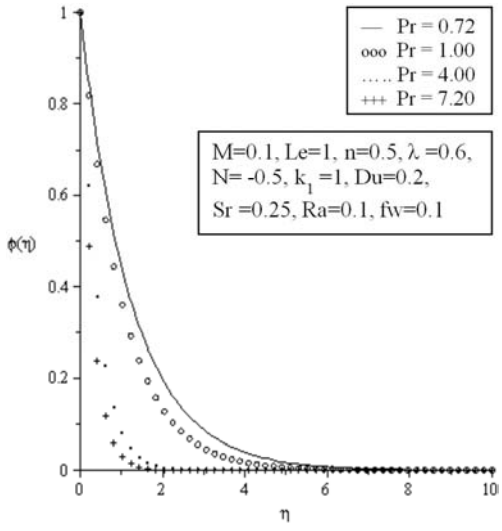

Figure 19. *Concentration profiles for varying values of Prandtl number (Pr).*

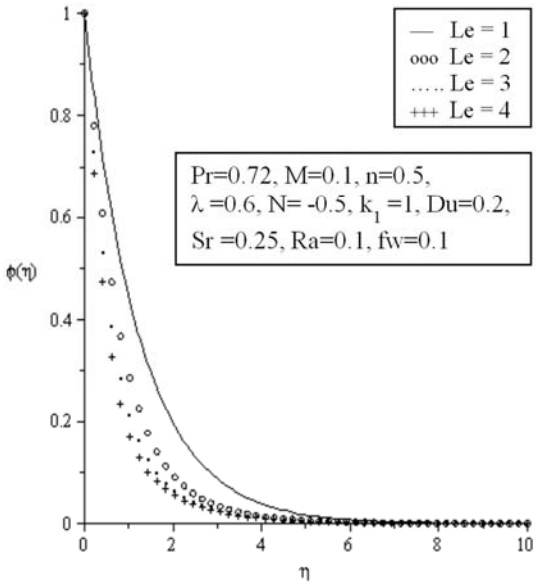

Figure 20. *Concentration profiles for varying values of Lewis number (Le).*

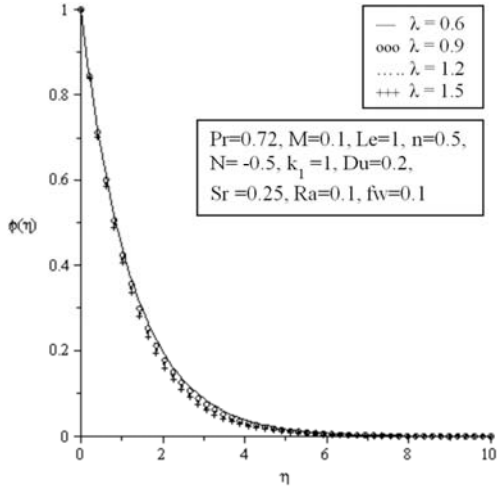

Figure 21. *Concentration profiles for varying values of buoyancy parameter (λ).*

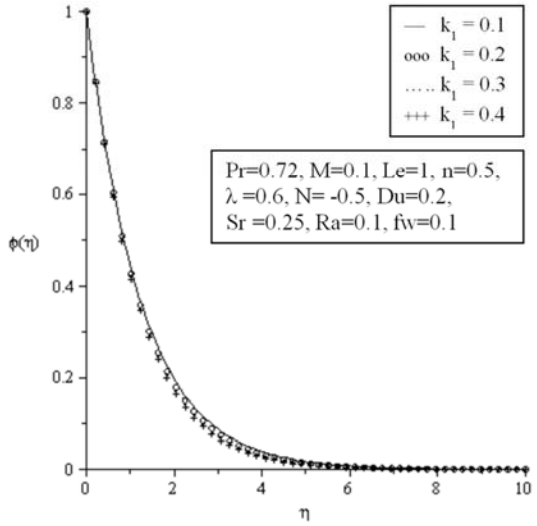

Figure 22. *Concentration profiles for varying values of viscoelasticity parameter (k_1).*

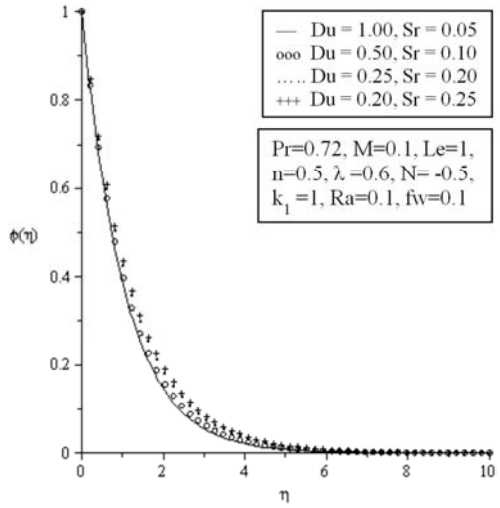

Figure 23. *Concentration profiles for varying Dufour (Du) and Soret (Sr) numbers.*

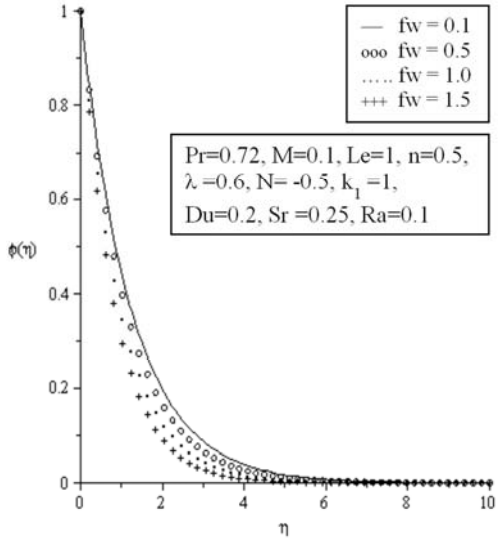

Figure 24. *Concentration profiles for varying values of Suction parameter (fw).*

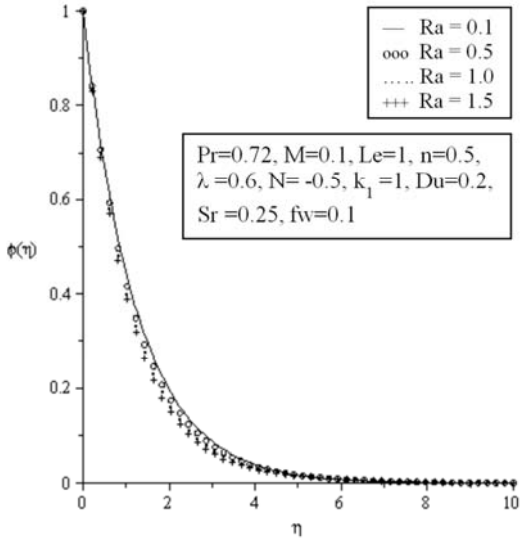

Figure 25. *Concentration profiles for varying values of radiation parameter (Ra).*

6. Summary of Findings

The comprehensive solutions have been obtained and presented in figures and tables. The numerical problem has one independent variable, three dependent fluid dynamic variables, and nine thermo physical parameters. The presentation indicates a perfect agreement. The equations governing fluid flow in general was derived and based on some assumptions, a mathematical model was developed for the problem under study and the associated boundary conditions. These models included the momentum, energy and species concentration equations which were nonlinear partial differential equations of higher order whose solution was not readily available. To make these coupled partial differential equations solvable numerically, similarity analysis was employed which reduced the problem to a set of nonlinear ordinary differential equations. These nonlinear ordinary differential equations which revealed the dimensionless parameters were solved by the Runge-Kutta integration along with the Newton Raphson algorithm using Maple 16 software.

The findings pointed to the increase in the skin friction as a result of intensifying the magnetic field strength as opposed to increasing buoyancy forces, radiation, and viscoelasticity.

7. Conclusion

Chemically MHD heat and mass transfer in viscoelastic fluid over vertical sheet with suction in the presence of Soret and Dufour effects and radiation have been investigated. Among all others we conclude that:

i. The combined effect of the induced Lorenz force, and suction increased the local skin friction; whereas combined effect of buoyancy forces, radiation, and viscoelasticity decreased it.
ii. The heat transfer rate increased with Soret and Dufour effects, suction and buoyancy; and reduced with radiation and viscoelasticity.
iii. The mass transfer rate increased with viscoelasticity; and decreased with Soret and Dufour effects.
iv. The velocity decreased with increasing the magnetic intensity due the drag in terms of a Lorentz force which resists the flow.

References

[1] Emmanuel, M. A., Ibrahim Y. S. and Letis B. B. (2015). Analysis of Casson Fluid Flow over a Vertical Porous Surface Chemical Reaction in the presence of Magnetic Field. Journal of Applied Mathematics and Physics, 3, 713-723.

[2] Andersson, H. I. (1992). MHD flow of a viscoelastic fluid past a stretching surface. *Acta Mech.*, 95, 227-230.

[3] Abel, S. P., Veena, H., Rajgopal, K. and Pravin, V. K. (2004). Non-Newtonian Magneto Hydrodynamic Flow over a Stretching Surface with Heat and Mass Transfer, Int. J. of Nonl. Mech., 39, 1067-1078.

[4] Abel, S. and Mahesha, N. (2008). Heat Transfer in MHD Viscoelastic Fluid Flow over a Stretching Sheet with Variable Thermal Conductivity, Non-Uniform Heat Source and Radiation, App. Math. Mod., 32, 1965-1983.

[5] Prasad, K. V., Pal, D., Umesh, V. and PrasannaRao, N. S. (2010). The Effect of Variable Viscosity on MHD Viscoelastic Fluid Flow and Heat Transfer over a Stretching Sheet, Com. in Nonl. Sc. and Num. Sim., 15 (2), 331-344.

[6] Kim, Y. J. (2000). Unsteady MHD convective heat transfer past a semi-infinite vertical porous moving plate with variable suction. *Int. J. Eng. Sci.*, 38, 833-845.

[7] Chamkha, A. J. and Khaled, A. R. A. (2001). Similarity solutions for hydromagnetic simultaneous heat and mass transfer by natural convection from an inclined plate with internal heat generation or absorption. *Heat Mass Transfer*, 37, 117-123.

[8] Seddeek, M. A. (2001). Thermal Radiation and Buoyancy Effect on MHD Free Convection Heat Generation Flow over an Accelerating permeable Surface With temperature dependent viscosity. *Can. J. Phys*., 79, 725-732.

[9] Aify, A. A. (2009). Similarity solution in MHD: effects of thermal dif-fusion and diffusion thermo on free convective heat and mass transfer over a stretching surface considering suction or injection, Comm. in Nonl. Sc. and Num. Sim., 14 (5), 2202–2214.

[10] Ouaf, M. E. M. (2005). Exact solution of thermal radiation on MHD flow over a stretching porous sheet. *Appl. Math. Comput.*, 170, 1117-1125.

[11] Cortell, R. (2006). Flow and heat transfer of an electrically conducing fluid of second grade over a stretching sheet subject to suction and to a transverse magnetic field. *Int. J. Heat Mass Transfer*, 49, 1851–1856.

[12] Subhas, M. A., Sanjayanand, E. and Nandeppanavar, M. M. (2007). Viscoelastic MHD flow and heat transfer over a stretching sheet with viscous and Ohmic dissipation. *Communications in Nonlinear Science and Numerical Simulation*, 13, 1808-1821.

[13] Barletta, A. and Celli, M. (2007). Mixed convection MHD flow in a vertical channel: Effects of Joule heating and viscous dissipation. *International Journal of Heat and Mass Transfer*, 51, 6110-6117.

[14] Ahmed, N., Sarma, K. and Ahmed, S. (2007). Free and Forced convective MHD flow and mass transfer through a porous medium bounded by an infinite vertical porous plate in the presence of a constant heat flux and heat source. *Proc. of 52nd Congress of ISTAM, BNMIT, Bangalore*, December 14-17, 152-160.

[15] Pramanik, S. (2014). Casson Fluid Flow and Heat Transfer Past an Exponentially Porous Stretching Surface in Presence of Thermal Radiation. Ain Shams Eng. J. 5, 205–212.

[16] Mohammad, A. Md. Shah. A., Md. Rashedul, I., Md. Abdul A. and Md. Mahmud A. (2015) Magnetohydrodynamic Boundary Layer Flow of Non-Newtonian Fluid and Combined Heat and Mass Transfer about an Inclined Stretching Sheet. *Open Journal of Applied Sciences, 2015, 5, 279-294*.

[17] Krishnendu, B., Uddin, M. S., Layek, G. C. (2016). Exact solution for thermal boundary layer in Casson fluid flow over permeable shrinking sheet with variable wall temperature and thermal Radiation. *Alexandria Engineering Journal 55, 1703–1712.*

[18] Bhattacharyya, K. (2013) Boundary Layer Stagnation-Point Flow of Casson Fluid and Heat Transfer towards a Shrinking/Stretching Sheet. *Frontiers in Heat and Mass Transfer* (*FHMT*), 4, Article ID: 023003. http://dx.doi.org/10.5098/hmt.v4.2.3003.

[19] Eswara Rao, M. and Sreenadh, S. (2017). MHD Boundary Layer Flow of Casson Fluid Over a Stretching/Shrinking Sheet through Porous Medium. *Chemical and Process Engineering Research* ISSN 2224-7467 (Paper) ISSN 2225-0913 (Online) Vol. 47, 2017.

[20] Stefan G. E. L. and Ron A. J. V (2019). Hydrodynamic Lubrication Theory For An Exact Bingham Plastic Fluid Model. 46th Leeds-Lyon Symposium on Tribology - September 2-4, 2019, Lyon, France.

[21] Norihan Md, A., Rusya I. Y. and Siti S. P. M. I.(2018) Stability Analysis on Magnetohydrodynamic Flow of Casson Fluid over a Shrinking Sheet with Homogeneous-Heterogeneous Reactions Entropy 2018, 20, 652; doi: 10.3390/e20090652.

[22] Hassan, A. (2019). An improved particle shifting technique for incompressible smoothed particle hydrodynamics method. *International journal for numerical methods in fluids https://doi.org/10.1002/fld.4737*.

[23] Ahmed, A. A and El-Aziz, M. A. (2019). MHD Casson Fluid Flow over a Stretching Sheet with Entropy Generation Analysis and Hall Influence. Entropy, 21, 592; doi: 10.3390/e21060592.

[24] Rashidi, S., Maziar, D., Ellahi, R. Riaz, M. and Jamal-Abad, MT. Study of stream wise transverse magnetic fluid flow with heat transfer around an obstacle embedded in a porous medium. *Journal of magnetic and magnetic materials*. 378, 1128-137.